OpenHolo Algorithm Guide

(Reconstruction :: Wave Aberration)

Min-Sik Park

OpenHolo Commission

Contents

1. Introduction

A holographic display based on a viewing window enables the converging of a reconstruction wave into a viewing window by means of an optical system. Accordingly, a user can observe a reconstructed hologram image, even with a small diffraction angle. It is very difficult to manufacture an optical system with no aberrations; thus, it is inevitable that a certain amount of wave aberrations will exist. A viewing-window-based holographic display, therefore, always includes distortions in an image reconstructed from a hologram pattern. Compensating the distortions of a reconstructed image is a very important technical issue because it can dramatically improve the performance when reconstructing a digital three-dimensional content image from a hologram pattern. We therefore propose a method for suppressing image distortion by measuring and compensating the wave aberration calculated from a Zernike polynomial, which can represent arbitrary wave aberrations. Through our experimental configuration using only numerical calculations,

A holographic digital display provides users with a realistic three-dimensional (3D) image or video by manipulating the hologram pattern, which represents the wave field of a 3D object. A spatial light modulator (SLM), a core device of a holographic digital display, loads a hologram pattern to reconstruct a 3D object in a free space. An SLM such as a liquid crystal display (LCD), digital micro-mirror device (DMD), or liquid crystal on silicon (LCoS) can be implemented as a display panel. Existing commercial panels do not satisfy SLM performance with a wide-viewing zone angle to observe a reconstructed image from the hologram displayed on the SLM with the naked eye. This is because the current state of technology does not enable the manufacturing of a display panel with a sub-micro-pixel pitch. Several alternative approaches exist to address the limited viewing zone angle of an existing SLM using scanning multiplexing [1], [2], tiling multiplexing [3]-[5], and a viewing window [6], [7].

Among these methods, a holographic display based on a viewing window allows even an LCD with a large pixel pitch to realize a sufficiently wide viewing angle. Such a display, however, has a disadvantage in that a reconstructed hologram is geometrically distorted by

wave aberrations that are introduced by the converging optical system for generating a viewing window [7]. The converging optical system in a viewing-window holographic display cannot avoid wave aberrations according to Siedel aberrations if it is designed and implemented using only spherical surfaces [8].

Studies have been conducted on exploiting a complex wave field phase [9]-[12] and applying an affine geometrical transformation to a hologram [13]-[17] to correct a distorted image numerically reconstructed from a hologram in the field of digital holography. We chose an approach to change the phase information from a hologram to compensate optical system wave aberrations in the viewing-window holographic display. The renowned approach to changing a phase is to use both a wavefront sensor (or an optical interferometer) that can quantitatively measure wave aberrations and a deformable mirror that controls a physical surface in a random form [18], [19].

The wave aberrations can be mathematically represented using Zernike polynomials [20],[21], that is, a set of orthonormal functions. Zernike polynomials can be obtained through a wave aberration measurement, such as a Shack-Hartmann sensor [22] and interferometry [23]. A Shack-Hartmann sensor consists of a two-dimensional (2D) lenslet array and a charge-coupled device (CCD) sensor. Interferometry includes a reference optical system to generate a reference wave for interfering with an object wave propagated from a test optical system. A viewing-window holographic display is generally composed of a converging optical system with a large aperture to illuminate a large-sized SLM. The effective area of a Shack–Hartmann sensor is too small for measuring such a large aperture. Moreover, interferometry incurs a significant expense and effort for preparing a large-sized reference optical system. The measured wave aberrations of an optical system are compensated by a wave aberration compensator, such as a deformable mirror [24], [25] that can change its physical surface with an arbitrary shape. A wave aberration compensator also has a problem in handling a large aperture because its effective aperture is small, similar to a wave aberration measurement.

A method is therefore required for easily measuring and compensating wave aberrations with no limitation on the aperture size of a converging optical system in a viewing-window

holographic display. Ray tracing is very useful in measuring wave aberrations of an optical system with a large aperture because it can numerically calculate the Zernike coefficient from a given design specification of an optical system, even if a wave aberration measurement is not established. The obtained wave aberrations can be transformed into a compensation phase field, which is applied to a viewing-window holographic display [6],[7].

2. Algorithm

2.1. Wave Aberration Representation Method

A normalized Zernike polynomial $Z_n^m(\rho, \theta)$ composed of a normalization term N_n^m , a radial term $R_n^{|m|}(\rho)$ and a sinusoidal term $\varphi(\theta)$ is defined in (1) [10]. Here, ρ and θ indicate the radius and azimuthal angle, respectively, in polar coordinates, where θ is measured in a counterclockwise direction from the $+x$ axis. The subscript n and superscript m of Z indicate the order and frequency of a Zernike polynomial, respectively, where n is greater than or equal to zero, and the absolute value of m is less than or equal to n. Moreover, n and m are either odd or even.

$$Z_n^m(\rho, \theta) = \left\{ \begin{array}{l} N_n^m \times R_n^{|m|}(\rho) \times \cos(m\theta) \text{ for } m \geq 0 \\ -N_n^m \times R_n^{|m|}(\rho) \times \sin(m\theta) \text{ for } m < 0 \end{array} \right\} \quad (1)$$

The sinusoidal term in (1) is selected with a cosine function if the frequency m is greater than or equal to zero, and with a sine function for all other cases.

The radial term $R_n^{|m|}(\rho)$ is calculated according to (2), and is dependent on m, n, and ρ.

$$R_n^{|m|}(\rho) = \sum_{s=0}^{\frac{n-|m|}{2}} \frac{(-1)^s (n-s)!}{s! \left[\frac{(n+|m|)}{2} - s\right]! \left[\frac{n-|m|}{2} - s\right]!} \rho^{n-2s} \quad (2)$$

A Zernike polynomial consisting of both a radial term and a sinusoidal term is an orthogonal, not an orthonormal, function. It requires the additional term in (3) for normalization.

$$N_n^m = \sqrt{\frac{2(n+1)}{(1+\delta_{m,0})}} \quad (\delta_{m,0} = 1 \text{ if } m = 0, \delta_{m,0} = 0 \text{ if } m \neq 0) \quad (3)$$

The wave aberration function used to sum Zernike polynomial $Z_n^m(\rho, \theta)$ multiplied by coefficient W_n^m can represent any arbitrary wave aberration.

$$W(\rho, \theta) = \sum_{n=0}^{\infty} \sum_{m=-n}^{n} W_n^m Z_n^m(\rho, \theta) \quad (4)$$

In (5), Zernike polynomial coefficient W_n^m is obtained from an integral equation of the wave aberration function $W(\rho, \theta)$ multiplied by Zernike polynomial $Z_n^m(\rho, \theta)$.

$$W_n^m = \frac{1}{\pi} \int_0^1 \int_0^{2\pi} W(\rho, \theta) \cdot Z_n^m(\rho, \theta) d\theta \rho d\rho \quad (5)$$

The wave aberration field $P(\rho, \theta)$ is represented using the wave aberration function $W(\rho, \theta)$ in (6).

$$P(\rho, \theta) = e^{-j\frac{2\pi}{\lambda}W(\rho,\theta)} \quad \text{or}$$

$$P(x, y) = e^{-j\frac{2\pi}{\lambda}W(x,y)} \quad (6)$$

The polar coordinate (ρ, θ) can be converted into the Cartesian coordinate (x, y) by replacing (ρ, θ) with $\left(\sqrt{x^2 + y^2}, \tan^{-1}(y/x)\right)$.

Function Z=zernike_poly(n, m, x, y, d)	
Input	• n : highest order of the radial term (n > 0) • m : azimuthal frequency of the sinusoidal term (|m| <= n) • x : 1-D array of pupil x-coordinate values (length(x) = length(y)) • y : 1-D array of pupil y-coordinate values (length(y) = length(x)) • d : Aperture diameter
Output	• Z : the Zernike polynomial term of (n, m)

```
function Z=zernike_poly(n,m,x,y,d)

% initialize circular aperture function
x_max=length(x);
y_max=length(y);
radius=d/2;

for i=1:x_max
    for j =1:y_max
        A(i,j)=(sqrt(x(i)^2+y(j)^2) <= radius);
    end
end

% Calculate Normalization term
N=sqrt(2*(n+1)/(1+(m==0)));

% Calculate Zernike polynomial
if n==0
    Z=A;
else
    Z=zeros(x_max,y_max);
    for i=1:x_max
        for j=1:y_max
            r=sqrt(x(i)^2+y(j)^2);
            if (x(i)>=0 & y(j)>=0) | (x(i)>=0 & y(j)<0)
                theta=atan(y(j)/(x(i)+1e-30));
            else
                theta=pi+atan(y(j)/(x(i)+1e-30));
            end
            for s=0:(n-abs(m))/2
                Z(i,j)=Z(i,j)+(-1)^s*factorial(n-s)*(r/radius)^(n-2*s)/...
                    (factorial(s)*factorial((n+abs(m))/2-s)*factorial((n-abs(m))/2-s));
            end
            Z(i,j)=A(i,j)*N*Z(i,j)*((m>=0)*cos(m*theta)-(m<0)*sin(m*theta));
        end
    end
end
```

Line numbers shown: 1, 2, 3, 4, 5, 6

Code 1. Algorithm 2.1.1. Pseudo Code

2.1. Diffraction Model in Viewing-Window Holographic Display with Wave Aberration

The spherical wave field emitted from a point source functions as the reconstructed beam and illuminates the SLM plane through the converging optical system, which acts as a convex lens. The SLM modulates the spherical wave field according to a hologram pattern in order to reconstruct a 3D object in a free space. There are two kinds of modulated wave fields departing from the SLM plane. The first is a non-diffracted wave field in an on-axis hologram to be focused on one point on the pupil plane, which is located at a distance d_s away from the SLM plane. The other is a diffracted wave field of a zero order that is used to form a viewing window. A user can observe the reconstructed 3D object by placing an eye over the viewing window.
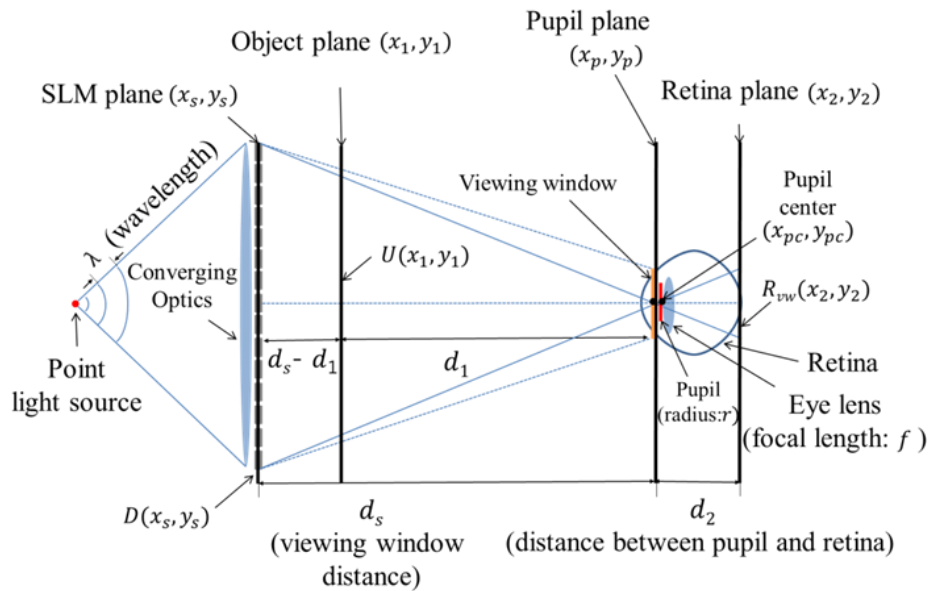

Fig. 1. Diffraction model based on a viewing window.

A wave field $D(x_s, y_s)$ on an SLM plane (x_s, y_s) as an input hologram propagates into a wave field $R(x_2, y_2)$ on a retina plane (x_2, y_2) through a wave field $U(x_1, y_1)$ on an

object plane (x_1, y_1). Here, $D(x_s, y_s)$ is a hologram pattern, a wave field inputted in the SLM plane of a holographic display; λ is defined as the wavelength of an illumination; d_1 is the distance between an object plane (x_1, y_1) and a pupil plane (x_p, y_p); d_2 is the distance between a pupil plane (x_p, y_p) and a retina plane (x_2, y_2); d_s is the distance between an SLM plane (x_s, y_s) and a retina plane (x_2, y_2); and f is the focal length of an eye lens.

The focal length f of an eye lens or a camera is calculated by (7), which is derived from the formula of the lens-maker if a user or camera focuses on an object plane (x_1, y_1) placed between the SLM plane (x_s, y_s) and retina plane (x_2, y_2).

$$\frac{1}{d_1} + \frac{1}{d_2} = \frac{1}{f}, \quad f = \frac{d_1 d_2}{d_1 + d_2} \qquad\qquad (7)$$

A pupil aperture function $PL(x_{pc}, y_{pc}, r)$ is defined with a circ function of (8), where (x_{pc}, y_{pc}) and r are the center coordinate and radius of the eye lens in the pupil plane, respectively. Here, $PL(x_{pc}, y_{pc}, r)$ is used to describe a situation in which an eye is shifted in the pupil plane.

$$PL(x_{pc}, y_{pc}, r) = circ\left\{ \frac{(x_p - x_{pc})^2 + (y_p - y_{pc})^2}{r^2} \right\}$$

$$= \begin{cases} 1 & \frac{(x_p - x_{pc})^2 + (y_p - y_{pc})^2}{r^2} < 1 \\ \frac{1}{2} & \frac{(x_p - x_{pc})^2 + (y_p - y_{pc})^2}{r^2} = 1 \\ 0 & \frac{(x_p - x_{pc})^2 + (y_p - y_{pc})^2}{r^2} > 1 \end{cases} \qquad (8)$$

The converging optical system generates the converging spherical wave field $S(x_s, y_s)$

with focal length d_s , as defined in (9).

$$S(x_s, y_s) = \exp\left\{-j\frac{2\pi}{\lambda}\frac{(x_s{}^2 + y_s{}^2)}{2d_s}\right\} \qquad (9)$$

The wave field $R_{vw}(x_2, y_2)$ is obtained by multiplying $D(x_s, y_s)$ by $S(x_s, y_s)$. The term $S(x_s, y_s)\exp\left\{j\frac{2\pi}{\lambda}\frac{(x_s{}^2+y_s{}^2)}{2d_s}\right\}$ in the second integral of (10) becomes one. Equation (10) represents the diffraction relationship between a wave field $R_{vw}(x_2, y_2)$ and a hologram pattern $D(x_s, y_s)$ in a viewing-window holographic display.

$$
\begin{aligned}
R_{vw}(x_2, y_2) = {} & \exp\left\{j\frac{2\pi}{\lambda}\frac{(x_2{}^2 + y_2{}^2)}{2d_2}\right\} \\
& \times \iint\limits_{-\infty}^{\infty} PL(x_{pc}, y_{pc}, r)\exp\left\{j\frac{2\pi}{\lambda}\left(\frac{1}{d_s} + \frac{1}{d_2} - \frac{1}{f}\right)\left(\frac{x_p{}^2 + y_p{}^2}{2}\right)\right\} \\
& \times \left[\iint\limits_{-\infty}^{\infty} D(x_s, y_s)S(x_s, y_s)\exp\left\{j\frac{2\pi}{\lambda}\frac{(x_s{}^2 + y_s{}^2)}{2d_s}\right\} \right. \\
& \left. \times \exp\left\{-j2\pi\left(\frac{x_p}{\lambda d_s}x_s + \frac{y_p}{\lambda d_s}y_s\right)\right\}dx_s dy_s \right] \\
& \times \exp\left\{-j2\pi\left(\frac{x_2}{\lambda d_2}x_p + \frac{y_2}{\lambda d_2}y_p\right)\right\}dx_p dy_p \qquad (10)
\end{aligned}
$$

For back-propagation from the wave field $R_{vw}(x_2, y_2)$ through the pupil plane, $D(x_s, y_s)$ is derived as (11).

$$D(x_s, y_s) = S(x_s, y_s)^{-1}\exp\left\{-j\frac{2\pi}{\lambda}\frac{(x_s{}^2 + y_s{}^2)}{2d_s}\right\}$$

$$\times \iint\limits_{-\infty}^{\infty} \exp\left\{-j\frac{2\pi}{\lambda}\left(\frac{1}{d_s} + \frac{1}{d_2} - \frac{1}{f}\right)\frac{(x_p{}^2 + y_p{}^2)}{2}\right\}$$

$$\times \left[\iint\limits_{-\infty}^{\infty} R_{vw}(x_2, y_2)\exp\left\{-j\frac{2\pi}{\lambda}\frac{(x_2{}^2 + y_2{}^2)}{2d_2}\right\}\right.$$

$$\times \exp\left\{j2\pi\left(\frac{x_p}{\lambda d_2}x_2 + \frac{y_p}{\lambda d_2}y_2\right)\right\} dx_2 dy_2 \right]$$

$$\times \exp\left\{j2\pi\left(\frac{x_s}{\lambda d_s}x_p + \frac{y_s}{\lambda d_s}y_p\right)\right\} dx_p dy_p \qquad (11)$$

Here, the term $S(x_s, y_s)^{-1}\exp\left\{-j\frac{2\pi}{\lambda}\frac{(x_s{}^2 + y_s{}^2)}{2d_s}\right\}$ of (11) is equal to one. The wave field $R_{vw}(x_2, y_2)$ can be replaced with the wave field $U\left(-\frac{d_1}{d_2}x_2, -\frac{d_1}{d_2}y_2\right)$ scaled down $U(x_1, y_1)$ by d_2/d_1 in the x and y axis direction according to (13), which is derived from the diffraction relationship between $R_{vw}(x_2, y_2)$ and $U(x_1, y_1)$ of (10) if equation (7) is satisfied.

$$R_{vw}\left(x_2, y_2; f = \frac{d_1 d_2}{d_1 + d_2}\right) = \exp\left\{j\frac{2\pi}{\lambda}\frac{(x_2{}^2 + y_2{}^2)}{2d_2}\right\}U\left(-\frac{d_1}{d_2}x_2, -\frac{d_1}{d_2}y_2\right)(12)$$

We can obtain $R_{vw}(x_2, y_2; f)$ according to (12) if an object wave field $U(x_1, y_1)$ is given and is focused by an eye or camera lens. In addition, $D(x_s, y_s)$ is furthermore generated by substituting the obtained $R_{vw}(x_2, y_2; f)$ in (11), and is the hologram pattern to be loaded on the SLM plane to optically reconstruct the object wave field $U(x_1, y_1)$.

The off-axis wave field is useful for enabling a reconstructed 3D object to be easily observed because it can spatially separate the twin hologram images to be reconstructed when SLM modulates only the amplitude of a complex wave field. The off-axis wave field $D_{shift}(x_s, y_s)$ on the SLM plane can be generated according to (13) by multiplying $D(x_s, y_s)$

by a shifting phase factor $SPF(x_s, y_s) = \exp\left\{j\frac{2\pi}{\lambda}\left(\sin\theta_{x_s} x_s + \sin\theta_{y_s} y_s\right)\right\}$. The shifting

phase factor $SPF(x_s, y_s)$ is equal to that introduced by a prism with deflection angle

$(\theta_{x_s}, \theta_{y_s})$ calculated from $\left(\tan^{-1}\frac{x_{pc}}{d_s}, \tan^{-1}\frac{y_{pc}}{d_s}\right)$ [27].

.

$$D_{shift}(x_s, y_s) = D(x_s, y_s) \times SPF(x_s, y_s) \qquad (13)$$

$SPF(x_s, y_s)$ is defined in (14) when a shifting coordinate is equal to (x_{pc}, y_{pc}), which is

the center coordinate of an eye lens in the pupil plane. $\left(\sin\left(\tan^{-1}\frac{x_{pc}}{d_s}\right), \sin\left(\tan^{-1}\frac{y_{pc}}{d_s}\right)\right)$

is approximately equal to $\left(\frac{x_{pc}}{d_s}, \frac{y_{pc}}{d_s}\right)$ assuming that d_s is greater than x_{pc} and y_{pc}.

$$SPF(x_s, y_s) = \exp\left\{j\frac{2\pi}{\lambda}\left(\frac{x_{pc}}{d_s}x_s + \frac{y_{pc}}{d_s}y_s\right)\right\} \qquad (14)$$

The converging optical system always includes some wave aberrations because it cannot be

optically designed with no such aberrations. It produces a converging spherical wave field

with wave aberrations for an illumination of a viewing-window holographic display. The

illumination wave field $C(x_s, y_s; x_{vc}, y_{vc})$ can be mathematically expressed as a

multiplication of both $S(x_s, y_s)$ and $P(x_s, y_s; x_{vc}, y_{vc})$ in (15).

$$C(x_s, y_s; x_{vc}, y_{vc}) = S(x_s, y_s) \times P(x_s, y_s; x_{vc}, y_{vc}) \qquad (15)$$

Here, $P(x_s, y_s; x_{vc}, y_{vc})$ is a wave aberration field on the SLM plane (x_s, y_s), calculated

according to (6), when a viewing window is centered at a coordinate (x_{vc}, y_{vc}) in the pupil

plane. The wave field leaving from the SLM plane is calculated by multiplying

$D_{shift}(x_s, y_s)$ by $C(x_s, y_s; x_{vc}, y_{vc})$. Thus, the retina wave field $R'_{vw}(x_2, y_2; x_{vc}, y_{vc})$ in a

viewing-window holographic display with wave aberrations is derived by replacing

$D(x_s, y_s)$ and $\exp\left\{j\frac{2\pi}{\lambda}\left(\frac{1}{d_s} + \frac{1}{d_2} - \frac{1}{f}\right)\left(\frac{x_p{}^2 + y_p{}^2}{2}\right)\right\}$ with $D_{shift}(x_s, y_s) \times C(x_s, y_s; x_{vc}, y_{vc})$

and $\exp\left\{j\frac{2\pi}{\lambda}\left(\frac{1}{d_s} + \frac{1}{d_2} - \frac{1}{f}\right)\left(\frac{(x_p - x_{pc})^2 + (y_p - y_{pc})^2}{2}\right)\right\}$.

$$R'_{vw}(x_2, y_2; x_{vc}, y_{vc}) = \exp\left\{j\frac{2\pi}{\lambda}\frac{(x_2{}^2 + y_2{}^2)}{2d_2}\right\}$$

$$\times \iint_{-\infty}^{\infty} PL(x_{pc}, y_{pc}, r)\exp\left\{j\frac{2\pi}{\lambda}\left(\frac{1}{d_s} + \frac{1}{d_2} - \frac{1}{f}\right)\left(\frac{(x_p - x_{pc})^2 + (y_p - y_{pc})^2}{2}\right)\right\}$$

$$\times \left[\iint_{-\infty}^{\infty} D_{shift}(x_s, y_s)P(x_s, y_s; x_{vc}, y_{vc})\exp\left\{-j2\pi\left(\frac{x_p}{\lambda d_s}x_s + \frac{y_p}{\lambda d_s}y_s\right)\right\}dx_s dy_s\right]$$

$$\times \exp\left\{-j2\pi\left(\frac{x_2}{\lambda d_2}x_p + \frac{y_2}{\lambda d_2}y_p\right)\right\}dx_p dy_p \qquad\qquad (16)$$

Equation (16) is used to calculate a wave field on the retina plane if a hologram pattern $D(x_s, y_s)$ on the SLM plane and a wave aberration field $P(x_s, y_s; x_{vc}, y_{vc})$ on the converging optical system is given. This means that (16) enables us to numerically reconstruct a hologram pattern on the SLM plane in a viewing-window holographic display with wave aberrations without conducting any optical experiments.

The hologram pattern $\bar{D}(x_s, y_s ; x_{vc}, y_{vc})$ of the compensating wave aberrations is generated by multiplying $D(x_s, y_s)$ by the inverse of a wave aberration field in (6) to suppress a wave aberration field $P(x_s, y_s ; x_{vc}, y_{vc})$ on the converging optical system when the center of the viewing window is placed at (x_{vc}, y_{vc}) in the pupil plane.

$$\bar{D}(x_s, y_s; x_{vc}, y_{vc}) = D_{shift}(x_s, y_s) \times P(x_s, y_s; x_{vc}, y_{vc})^{-1}$$
$$= D(x_s, y_s) \times SPF(x_s, y_s) \times P(x_s, y_s; x_{vc}, y_{vc})^{-1} \qquad (17)$$

Here, $\bar{D}(x_s, y_s ; x_{vc}, y_{vc})$ is derived in (18) with regard to $U\left(-\frac{d_1}{d_2}x_2, -\frac{d_1}{d_2}y_2\right)$ by

substituting $D(x_s,\ y_s)$ of (11) and $R_{vw}(x_2,\ y_2)$ of (12) in (16) if an object wave field $U(x_1,\ y_1)$ is given.

$$\overline{D}(x_s,y_s;x_{vc},y_{vc}) = SPF(x_s,\ y_s) \times P(x_s,y_s;x_{vc},y_{vc})^{-1}$$

$$\times \iint\limits_{-\infty}^{\infty} \exp\left\{-j\frac{2\pi}{\lambda}\left(\frac{1}{d_s}+\frac{1}{d_2}-\frac{1}{f}\right)\frac{(x_p{}^2+y_p{}^2)}{2}\right\}$$

$$\times\left[\iint\limits_{-\infty}^{\infty} U\left(-\frac{d_1}{d_2}x_2,-\frac{d_1}{d_2}y_2\right)\exp\left\{j2\pi\left(\frac{x_p}{\lambda d_2}x_2+\frac{y_p}{\lambda d_2}y_2\right)\right\}dx_2 dy_2\right]$$

$$\times \exp\left\{j2\pi\left(\frac{x_s}{\lambda d_s}x_p+\frac{y_s}{\lambda d_s}y_p\right)\right\}\ dx_p dy_p \qquad\qquad (18)$$

Equations (16) and (18) can be represented through a Fourier transform to employ a fast Fourier transform (FFT).

$$R'_{vw}\ (x_2,\ y_2;x_{vc},y_{vc})$$

$$= \exp\left\{j\frac{2\pi}{\lambda}\frac{(x_2{}^2+y_2{}^2)}{2d_2}\right\}FT_{(x_p,y_p)}\left[PL(x_{pc},y_{pc},r)\exp\left\{j\frac{2\pi}{\lambda}\left(\frac{1}{d_s}+\frac{1}{d_2}\right.\right.\right.$$

$$\left.\left.-\frac{1}{f}\right)\left(\frac{(x_p-x_{pc})^2+(y_p-y_{pc})^2}{2}\right)\right\}$$

$$\times FT_{(x_s,y_s)}\{D(x_s,\ y_s)SPF(x_s,\ y_s)P(x_s,y_s;x_{vc},y_{vc})\}\Big] \qquad (19)$$

$$\overline{D}(x_s,y_s;x_{vc},y_{vc}) =\ SPF(x_s,\ y_s)P(x_s,y_s;x_{vc},y_{vc})^{-1}$$

$$\times FT^{-1}_{(x_p,y_p)}\left[\exp\left\{-j\frac{2\pi}{\lambda}\left(\frac{1}{d_s}+\frac{1}{d_2}-\frac{1}{f}\right)\frac{(x_p{}^2+y_p{}^2)}{2}\right\}\right.$$

$$\times FT^{-1}_{(x_2,y_2)}\left\{U\left(-\frac{d_1}{d_2}x_2,-\frac{d_1}{d_2}y_2\right)\right\}\Big] \qquad\qquad (20)$$

Here, $(\overline{D}(x_s, y_s \ ; x_{vc}, y_{vc})$ is the hologram pattern to be generated with respect to the single depth between the SLM plane and the object plane.

The 3D object consists of sliced object planes with different depths. The compensated volume hologram pattern $\overline{\overline{D}}(x_s, y_s; x_{vc}, y_{vc})$ is obtained as the sum of the hologram patterns generated with regard to the sliced object planes, as shown in Fig. 2. The value of $\overline{\overline{D}}(x_s, y_s; x_{vc}, y_{vc})$ is calculated according to (21) if a 3D object is divided with N-sliced object planes.

$$\overline{\overline{D}}(x_s, y_s; x_{vc}, y_{vc}) = \sum_{i=1}^{N} \overline{D}(x_s, y_s; x_{vc}, y_{vc}, z_i) \qquad (21)$$
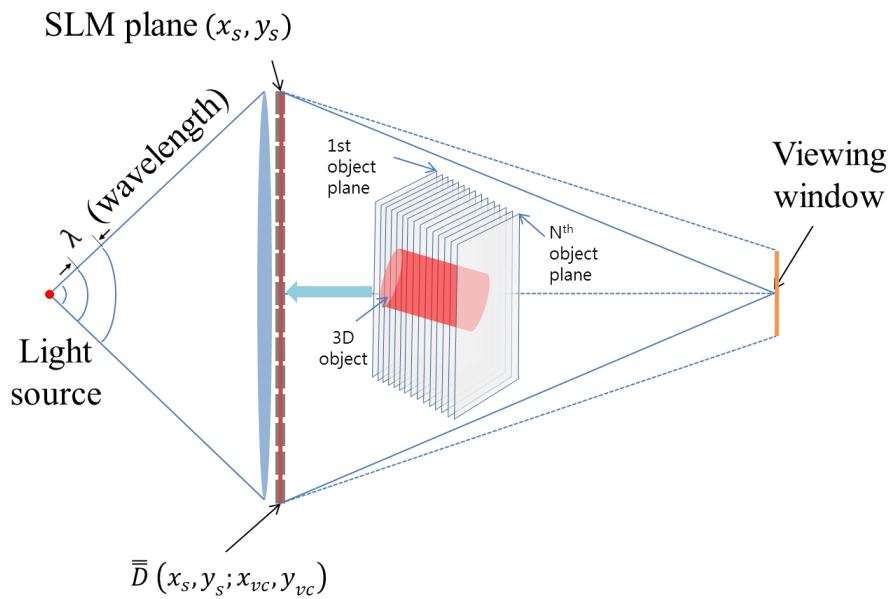

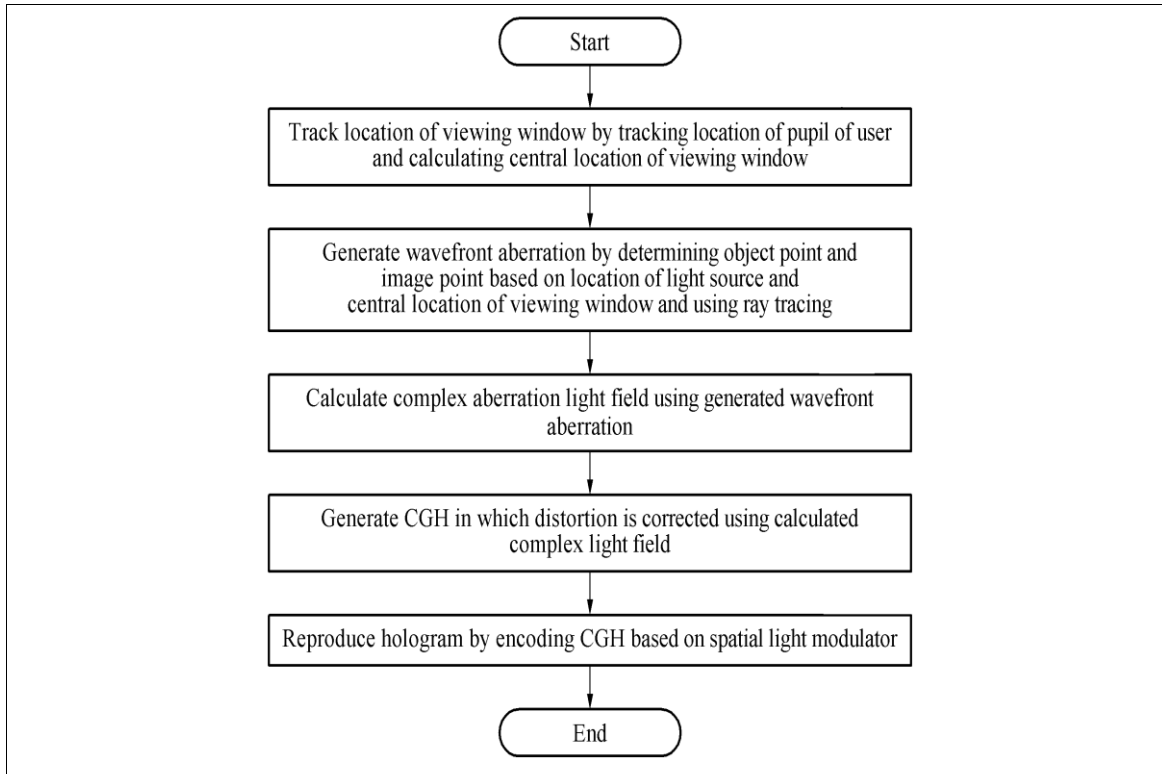Fig. 2. Hologram pattern generation in a 3D object.

Fig 1. Algorithm 2.1.2. Flow Chart

3. Implementation S/W

3.1. Wave Aberration Representation Method

Type	Source File	S/W	Description
Matlab	*zernike_poly.m*		This function computes the values of a Zernike Polynomial over a circular pupil of diameter d

3.2. Diffraction Model in Viewing-Window

(TBD)

4. Glossary

(TBD)

5. Reference

[1] M. Stanley et al., "100 Mega-pixel computer generated holographic images from Active Tiling – a dynamic and scalable electro-optic modulator system," *Proc. SPIE-IS&T*, vol. 5005, pp. 247-258, 2003

[2] Y. Takaki and N. Okada, "Hologram generation by horizontal scanning of a high-speed spatial light modulator," *Applied Optics*, vol. 48, no. 17, pp.3255-3260, 2009

[3] J.K. Hahn et al., "Wide viewing angle dynamic holographic stereogram with a curved array of spatial light modulators," *Optics Express*, vol. 16, no. 16, pp. 12372-12386, 2008

[4] T. Kozacki et al., "Wide angle holographic display system with spatiotemporal multiplexing," Optics Express, vol. 20, no. 25, pp. 27473-27481, 2012

[5] J.-Y. Son et al., "Holographic display based on a spatial DMD array," *Optics Letter*, vol. 38, pp. 3173-3176, 2013

[6] S. Reichelt et al., "Holographic 3-D Displays- Elector-holography within the Grasp of Commercialization," INTECH, Chap. 29,   2010

[7] M. Park , B. G. Chae , H. Kim , J. Hahn , H. Kim , C. H. Park , K. Moon , J. Kim., "Digital holographic display system with large screen based on viewing window movement for 3D video service," *ETRI Journal*, vol. 36, no. 2, pp. 232-241, 2014

[8] E. Hecht, *Optics-4th edition*, A. Wesley, pp.253-266, 2002

[9] J. Upatnieks, A. Vander Lugt, and E. Leith, "Correction of Lens Aberrations by Means of Holograms," *Applied Optics,*   vol. 5, pp. 589-593 , 1966

[10] A. Stadelmaier and J. H. Massig, "Compensation of lens aberrations in digital holography," *Optics Letters*, vol. 25, pp. 1630–1632, 2000

[11] P. Ferraro, S. De Nicola, A. Finizio, G. Coppola, S. Grilli, C. Magro, and G. Pierattini ,"Compensation of the inherent wave front curvature in digital holographic coherent microscopy for quantitative phase-contrast imaging," *Applied Optics,*   vol. 42, pp. 1938-1946 , 2003

[12] T. Colomb et al., "A numerical parametric lens for shifting, magnification and complete aberration compensation in digital holographic microscopy," *J. Opt. Soc. Am. A* , vol. 23, pp. 3177-3190, 2006

[13] M. Paturzo and P. Ferraro, "Creating an extended focus image of a tilted object in Fourier digital holography," *Optics Express*, vol. 17, no. 22, pp. 20546-20552, 2009

[14] P. Ferraro, M. Paturzo, P. Memmolo and A. Finizio, "Controlling depth of focus in 3D image reconstructions by flexible and adaptive deformation of digital holograms," *Optics Letter*, vol. 34, pp. 2787-2789, 2009

[15] M. Paturzo, P. Memmolo, A. Finizio, R. Näsänen, T. J. Naughton and P. Ferraro, "Synthesis and display of dynamic holographic 3D scenes with real-world objects," *Optics Express*, vol. 18, no. 9, pp. 8806-8815, 2010

[16] P. Memmolo, C. Distante, M. Paturzo, A. Finizio, P. Ferraro, and B. Javidi., "Automatic focusing in digital holography and its application to stretched holograms," *Optics Letter*, vol. 36, pp. 1945-1947, 2011

[17] T. Shimobaba., M. Makowski, T. Kakue, M. Oikawa, N. Okada, Y. Endo, R. Hirayama, and T. Ito "Lensless zoomable holographic projection using scaled Fresnel diffraction," *Optics Express*, vol. 21, no. 21, pp. 25285-25290, 2013

[18] T. K. Uhm et.al. "A study on the actuator arrays of a deformable mirror for adaptive

optics," Optical Society of Korea, vol. 13(5), pp. 442-448, 2002

[19] Martin J Booth, "Adaptive optics in microscopy," Philosophical Transactions of the Royal Society, vol. 365, pp. 2829-2843, 2007

[20] H. Gross, *Handbook of Optical systems*, WILEY-VCH, vol. 2, pp. 212-216, 2007

[21] R. Navarro, R. Rivera, and J. Aportab, "Representation of wavefronts in free-form transmission pupils with Complex Zernike Polynomials," *J. Optom*, vol. 4, no. 2, pp. 41-48, 2011

[22] B. C. Platt and R. Shack, "History and principles of Shack-Hartmann wavefront sensing," *J. Refract. Surg.*, vol. 17, no. 5, pp. S573–S577, 2001

[23] H. Gross, *Handbook of Optical Systems*, WILEY-VCH, vol. 1, pp. 782-786, 2007)

[24] O. Cugat et al., "Deformable magnetic mirror for adaptive optics: technological aspects," *Sensors and Actuators A*, vol. 89, no. 1-2, pp. 1-9, 2001

[25] T. K. Uhm et al., "A study on the actuator arrays of a deformable mirror for adaptive optics," *Optical Society of Korea*, vol. 13, no. 5, pp. 442-448, 2002

[26] J. W. Goodman, *Introduction to Fourier Optics – 3rd edition*, Roberts & Company, pp. 109-115, 2005

[27] Etienne Cuche, Pierre Marquet, and Christian Depeursinge, "Spatial filtering for zero-order and twin-image elimination in digital off-axis holography," *Applied Optics*, vol. 39, no. 23, pp.4070-4075, 2000

[28] http://www.zemax.com/

[29] http://michel.thoby.free.fr/Fisheye_history_short/International_Standards_about_Distortion.html

[30] Y. Hao and A. Asundi, "Resolution analysis of a digital holography system," Applied Optics, vol. 50, no. 2, pp.183-193, 2011

[31] P. Ferraro, C. Del Core, L. Miccio, S. Grilli, S. De Nicola, A. Finizio, and G. Coppola, "Phase map retrieval in digital holography: avoiding the under sampling effect by a lateral shear approach," Proc. of SPIE, vol. 6995, pp. 6995061-6995066 , 2008